

# Static and dynamic study of composite beams with a new interlaminar sliding field using different beam theories

Rachida Mohamed Krachai<sup>a</sup>, Noureddine Elmeiche<sup>b</sup>,  
Ismail Mechab<sup>c</sup>, Fabrice Bernard<sup>d</sup>, Hichem Abbad<sup>e</sup>


<sup>a</sup> Djilali Liabes University, Faculty of Technology,  
Department of Civil Engineering and Public Works,  
Civil and Environmental Engineering Laboratory (LGCE),  
Sidi Bel-Abbes, People's Democratic Republic of Algeria +  
Mustapha Stambouli University, Faculty of Science and Technology,  
Department of Civil Engineering,  
Mascara, People's Democratic Republic of Algeria,  
e-mail: rm.kirachai@univ-mascara.dz,  
ORCID iD: <https://orcid.org/0009-0004-7530-433X>

<sup>b</sup> Djilali Liabes University, Faculty of Technology,  
Department of Civil Engineering and Public Works,  
Civil and Environmental Engineering Laboratory (LGCE),  
Sidi Bel-Abbes, People's Democratic Republic of Algeria,  
e-mail: noureddine.elmeiche@univ-sba.dz, **corresponding author**,  
ORCID iD: <https://orcid.org/0000-0002-6412-0840>

<sup>c</sup> Djilali Liabes University, Faculty of Technology,  
Department of Mechanical Engineering,  
Laboratory of Mechanics and Physics of Materials (LMPM),  
Sidi Bel-Abbes, People's Democratic Republic of Algeria,  
e-mail: ismail.mechab@gmail.com,  
ORCID iD: <https://orcid.org/0009-0004-4922-6980>

<sup>d</sup> University of Rennes, INSA Rennes,  
Civil and Mechanical Engineering Laboratory (LGCGM),  
Rennes, French Republic,  
e-mail: fabrice.bernard@insa-rennes.fr,  
ORCID iD: <https://orcid.org/0000-0001-7495-936X>

<sup>e</sup> Djilali Liabes University, Faculty of Technology,  
Department of Civil Engineering and Public Works,  
Civil and Environmental Engineering Laboratory (LGCE),  
Sidi Bel-Abbes, People's Democratic Republic of Algeria,  
e-mail: hi\_abbad@yahoo.fr,  
ORCID iD: <https://orcid.org/0000-0001-9896-5369>

 <https://doi.org/10.5937/vojtehg73-52773>

FIELD: civil engineering

ARTICLE TYPE: original scientific paper

## Abstract:

*Introduction/purpose: The present work aims to carry out a static and dynamic investigation of composite beams composed of two elements*

*connected together, with a partial interaction between the beam layers, while taking into account the interlaminar sliding effect.*

*Methods: A new interlaminar slip field which takes into account, for each layer, the axial displacement, the rotation due to bending, and the high-order transverse shear with a new warping shape function, has been introduced in this study. The equilibrium equations were solved analytically based on the principle of Hamilton. In addition, the numerical resolution of these equations was based on the principle of minimizing all energies using the Ritz method, while taking into account different beam theories. Afterwards, a comparative study was carried out in order to calculate the natural vibration frequencies of two composite beams made of steel and wood materials.*

*Results: It was found that the results obtained for the ten natural vibration frequencies are in perfect agreement with those reported in previous works found in the literature.*

*Conclusion: Further, a detailed study was conducted, depending on the geometric and material parameters, for the two mixed materials, i.e., concrete-wood and steel-concrete, with two interlaminar sliding fields, namely the classical sliding field based on the Timoshenko beam theory and a new interlaminar sliding field that is based on the high order theory. Furthermore, bending was studied in the static case in order to examine the effect of the interlaminar shear force on short and long beams.*

*Keywords: static and dynamic study, composite beams, partial interaction, new interlaminar slip field, high order transverse shear, new warping shape function, Ritz method.*

## Introduction

Sliding in mixed structures is a complex phenomenon that often occurs at the interface between two or more different materials, under the effect of variable static, dynamic or thermal stresses which may engender some deformation or critical damage. It should be noted that the connection between a concrete slab and a steel or wooden beam, for example, is generally ensured by shear connectors placed in the composite beams. The role of these connectors is to prevent the occurrence of shear at the interface, along the composite beam, which is subjected to a bending load. The interface is an essential element that plays an indispensable role in the behavior of the composite beam. Indeed, if the concrete slab and the beam are freely superimposed, then the two elements flex independently and considerable sliding occurs at their interface. Therefore, in order to reduce or eliminate this sliding, it is deemed appropriate to have a sufficient number of shear connectors at the interface between the slab and the beam. This technique allows

transferring the forces between the two materials, and therefore producing a mixed bending of one single element that is more resistant and has higher rigidity. It was revealed that numerous works have been carried out on the topic under study. Regarding Xu & Wu (2008), they examined the free vibration and buckling of composite beams with interlayer sliding based on a two-dimensional theory, and using semi-analytical solutions, under boundary conditions that were determined with a coupling between the Differential Quadrature method and the State Space method. As for Nguyen (2009), he developed numerical models that are capable of predicting the instantaneous and delayed behavior of composite steel-concrete beams. Similarly, Le Grogne et al. (2012) proposed an exact buckling solution for two-layer Timoshenko beams with interlayer slip. Likewise, Lenci & Clementi (2012) examined the effects of shear stiffness, rotary and axial inertia, and interface stiffness, on the free vibrations of a two-layer beam. With regard to Castel (2013), he presented a model that can be employed to describe the vibrational behavior of composite structures, i.e., plates that are partially covered with passive constrained layer damping (PCLD) patches that play the role of damping elements. He investigated the energy of the system under study using three different methods, namely the Rayleigh-Ritz method, the Navier method, and the finite element method. On the other hand, Galuppi & Royer-Carfagni (2014) investigated the buckling of three-layer composite beams with viscoelastic interaction. Furthermore, Čas et al. (2018) proposed an analytical solution to the two-layer three-dimensional composite beam with interlayer slips. Likewise, Perkowski & Czabak (2019) described the behavior of composite wood-concrete beams under hygrothermal loading. The two materials, i.e., wood and concrete, are linked by a joint. In this case, the eventual interlayer sliding and the joint uplift were taken into account in order to determine the rigidity of the composite beam and also to estimate the shrinkage/swelling that is due to humidity of wood and concrete in the long term. This allowed them to propose a model and formulate an inverse problem. As for Adam & Furtmüller (2020), they studied the bending vibrations of composite beams presenting geometric nonlinearities, and subjected to interlayer sliding. In addition, Santos (2020) analyzed the buckling of two-layer laminated composite beams, with interlayer sliding, using the finite element method. It should be noted that the geometrically nonlinear beam elements have a single flexible shear interface and each layer is modeled using the Timoshenko theory. Subsequently, the inter-element equilibrium as well as the Neumann boundary conditions was applied while using the Lagrangian multiplier method. On the other hand, Lemes et al. (2021) carried out a numerical

analysis of composite steel-concrete beams, with partial shear interaction, in order to theoretically determine two-dimensional displacement using the plastic-hinge approach. Moreover, Lemes et al. developed an effective numerical method for the purpose of analyzing mixed steel-concrete structures while taking into account the nonlinear geometric and material effects. Afterwards, a methodology based on the Refined Plastic Hinge Method (RPHM) was developed and the stiffness parameters were obtained by considering a homogeneous cross section of the structure. The strain compatibility method (SCM) was applied to evaluate the strength of structural elements. Likewise, the Newton-Raphson method was adopted to solve nonlinear global and local equations, at the cross section level. The results obtained were then compared with the others found in the experimental and numerical databases available in the literature (Lemes et al, 2017). With regard to Barbosa et al. (2019) they presented an experimental study with a view to developing a Truss connector in a mixed concrete-steel beam and also to analyzing the behavior of failure loads, the transverse displacements between concrete slabs, and the relative vertical sliding between the reinforced concrete slabs and the metal profiles of the developed models. Further, Yoo et al. (2021) presented a nonlinear analysis method to evaluate the bending behavior of a composite beam while taking into account partial interaction. They applied the Fourier series for the purpose of determining the shear interface forces in the composite beam while taking into consideration the sliding effect between steel and concrete, and by considering the inelastic behavior of the steel beam and the nonlinear behavior of the ultra-high performance fiber-reinforced concrete (UHPC). As for Honarvar et al. (2020), they examined the steel-concrete composite beam with bolt shear connectors. The composite beam was subjected to three different loading conditions, including pure bending loading and simultaneous bending loading, with two alternative torsional loading modes. The results obtained were analyzed using a 3D nonlinear finite element model. This study was aimed to carry out the analysis of the mid-span deflection, rotation and sliding of composite beams, under different loading conditions. In addition, the effect of the type and number of shear connectors on the sliding of the composite beam was also investigated.

The findings indicated that the slip between the steel beam and concrete slab, along the composite beam, increased in the direction of increasing bending load, while torsion load had a slight effect on sliding. In this context, Carvalho et al. (2021) developed two methods which are based on plane displacement with concentrated nonlinear effects for the numerical analysis of composite beams. It should be noted that the effects



of geometric nonlinearity, plasticity, and partial shear connection are taken into account. In the two approaches used, the co-rotational system is defined in such a way as to allow large displacements and rotations in the numerical model. The first method is based on the strain compatibility method. In this case, the deformations of the sections and the sliding at the steel-concrete interface are analyzed as well as the axial and bending rigidity of the cross section. The second approach is based on the finite element method in order to simulate plasticity. All the numerical results obtained by these two approaches turned out to be quite accurate. They are close to the experimental data reported in the literature (Carvalho et al, 2021). In this regard, Oliveira et al. (2021) carried out a study on the serviceability limit state of excessive deflections by adopting two simplified approaches, namely Eurocode 4:2004 (European code) and AS/NZS 2327:2017 (Australian code). The results obtained were compared with the experimental ones that have previously been reported by other authors in the literature. The occurrence of non-uniform shrinkage becomes a relevant aspect due to the impermeability of the face that is favored by the steel decking. Based on the above, it was deemed appropriate to neglect the deflections when Eurocode 4 was adopted. At the same time, the simplified AS/NZS 2327 approach, which explicitly takes into account non-uniform shrinkage, gave results that are more precise than those obtained by the experimental method. In addition, several studies were carried out using the First-order Shear Deformation Theory (FSDT) which applies in the case of short beams. This theory is based on the principle which states that after deformation the plane section remains plane but loses its perpendicularity with respect to the mean line of the beam. This is due to the transverse shear occurring through the thickness of the beam that was initially discovered by Timoshenko. The First-order Shear Deformation Theory (FSDT) is attributed to Reissner (1945) and Mindlin (1951) who developed the Reissner-Mindlin plate model. Other similar works, such as those carried out by Timoshenko & Woinowsky-Krieger (1959), Whitney (1969), Reddy (1984), Kant & Swaminathan (2001), Della Croce & Venini (2004), Wang et al. (2000), Valizadeh et al. (2013), Mechab (2005), also deserve to be mentioned.

The primary purpose of this investigation is to conduct an analytical and numerical study on free vibrations and the interlaminar bending shear force. For this, a new interlaminar sliding field of a composite beam was introduced. This field takes into account the axial displacements, rotations, as well as the warping effect of the section of the two composite beams. Furthermore, a new transverse shear strain shape function was introduced in order to see the transverse shear influence of short beams. For this, two

types of composite beams were studied, i.e., one composite steel-wood beam and one steel-concrete beam. The numerical results were compared with the ones found in the literature and in other deformation theories.

## Equation of interlaminar slip between layers

### Balance of forces

Consider a composite beam composed of two different materials in partial connection (Figure 1). This beam is subjected to bending under uniformly distributed loading. Figure 2 shows the free-body diagram of an infinitesimal element of length  $dx$  of the composite beam subjected to an external force distributed along the element. The bending moment, the shear force, and the normal force are denoted by  $M$ ,  $Q$ , and  $N$ , respectively.

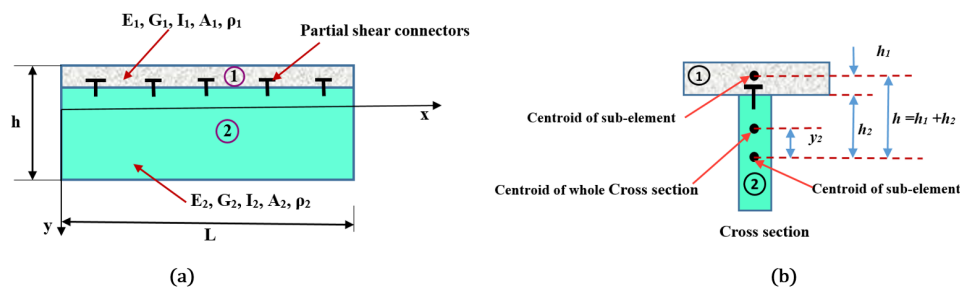


Figure1 – Composite member and the coordinate system; (a) elevation; (b) cross-section

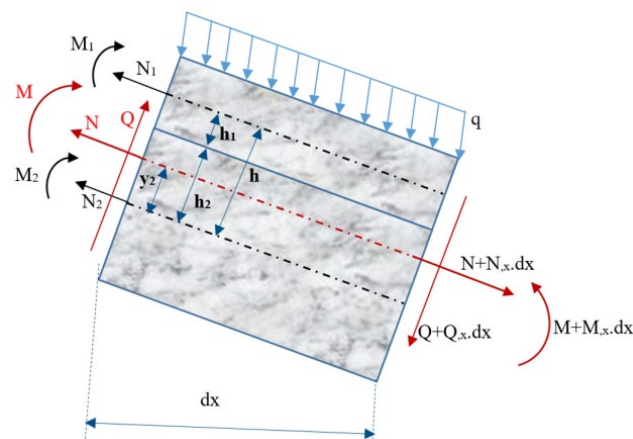


Figure 2 – Internal forces acting on an infinitesimal element of the composite beam under bending

According to the small deformation hypothesis, the dynamic equilibrium equations of the force applied along the x and y directions and the bending moment can be expressed using the three equations given below:

$$N=F$$

Here, F is the applied axial force

$$\frac{dQ}{dx} = q + \bar{\rho}A \frac{d^2v}{dt^2} - N \frac{d^2v}{dx^2}, \quad \frac{dM}{dx} = Q - \bar{\rho}I \frac{d^2\theta}{dt^2} \quad (1)$$

with

$$\bar{\rho}A = \rho_1 A_1 + \rho_2 A_2, \quad \bar{\rho}I = \rho_1 I_1 + \rho_2 I_2 \quad (2)$$

It should be noted that the small deformation hypothesis is part of the small disturbance hypothesis which is the combination of two hypotheses, namely the small deformation hypothesis and the small displacement hypothesis.

It is to be noted that  $N_1$ ,  $N_2$ ,  $M_1$  and  $M_2$  represent the axial forces and the bending moments for the two elements 1 and 2, respectively. In addition, the axial force  $N$  and the bending moment  $M$  of the entire section are assumed to be applied at the center of gravity of the solid composite section. Then, using the static equilibrium equations allows writing:

$$N = N_1 + N_2 = F$$

$$N_2 = F - N_1 \quad (3)$$

$$M = M_1 + M_2 - N_1 h + N y_2$$

Furthermore, the sliding at the interface between the two elements 1 and 2 is taken into account. Figure 3 clearly depicts the normal force applied on each element, including the shear force produced by the shear connectors, as well as the two normal forces  $N_1$  and  $N_2$ .

Hence, considering the equilibrium of forces in the axial direction helps to determine the shear force at the interface between the two elements as follows:

$$\frac{dN_1}{dx} = -\frac{dN_2}{dx} = -Q_s \quad (4)$$

The shear force  $Q_s$  between the two elements is then determined as:

$$Q_s = k_s u_s \quad (5)$$

where  $u_s$  denotes the slip filed between the two elements, and  $k_s$  is stiffness of the shear connector.

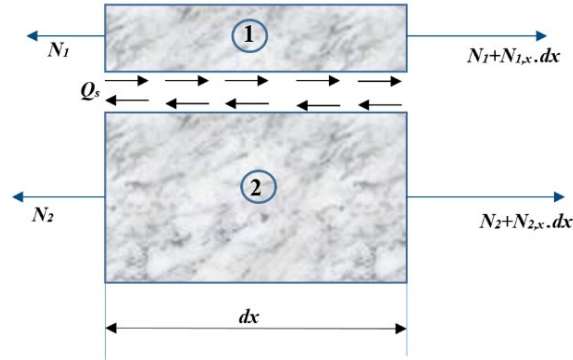


Figure 3 – Forces applied along the axial direction of the composite beam

### Kinematics of the interlaminar slip field

Considering Figure 4, and according to Timoshenko's hypothesis, the interlaminar sliding field  $u_s$  between the materials of the composite beam is a function of the longitudinal displacements of each element and the overall rotation of the beam. It can be expressed in the following form:

$$u_s = u_2(x, y) - u_1(x, y) + h_1 \cdot \theta(x) + h_2 \cdot \theta(x) \quad (6)$$

$$u_s = u_2(x, y) - u_1(x, y) + h \cdot \theta(x)$$

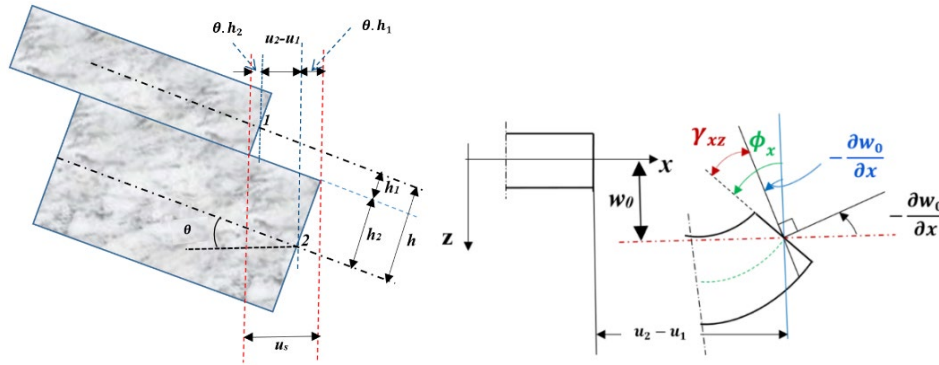


Figure 4 – Sliding diagram of the two elements, considering the Timoshenko beam theory

The interlayer shear strain may be determined by deriving equation 6 with respect to  $x$ , which gives:

$$\frac{du_s}{dx} = \frac{du_2(x, y)}{dx} - \frac{du_1(x, y)}{dx} + h \cdot \frac{d\theta(x)}{dx} \quad (7)$$

$$\frac{du_s}{dx} = \varepsilon_2 - \varepsilon_1 + h \cdot \frac{d\theta(x)}{dx}$$



where  $\varepsilon_1$ , and  $\varepsilon_2$  are the normal deformations, in the x direction, with respect to the centers of gravity of elements 1 and 2, respectively. They can be determined as:

$$u_{1,x}=\varepsilon_1=\frac{N_1}{E_1A_1}, u_{2,x}=\varepsilon_2=\frac{N_2}{E_2A_2} \quad (8)$$

Furthermore, the Timoshenko beam theory may be used to express the bending moment as follows:

$$M_1=E_1I_1\frac{d\theta}{dx}, M_2=E_2I_2\frac{d\theta}{dx}, \overline{kGA}=k_1G_1A_1+k_2G_2A_2 \quad (9)$$

Here  $k_1$  and  $k_2$  are the coefficients of the shear connectors used in the beam under study. They depend on the shape of the cross section of the elements of the composite beam.

Then, deriving equation (6) with respect to x gives:

$$u_{s,x}=u_{2,x}-u_{1,x}+h\cdot\theta(x),_x \quad (10)$$

Likewise, deriving equation (5) with respect to x leads to:

$$Q_{s,x}=k_s\cdot u_{s,x} \quad (11)$$

Next, equation (8) is substituted into equation (11) to get:

$$Q_{s,x}=k_s\cdot\left(\frac{N_2}{E_2A_2}-\frac{N_1}{E_1A_1}+h\cdot\theta(x),_x\right) \quad (12)$$

After derivation and some substitutions, the following differential equation is then obtained:

$$\begin{aligned} N_{1,xx} &= -N_{2,xx} = -Q_{s,x} \\ N_{1,xx} &= -k_s \cdot \left( \frac{F-N_1}{E_2A_2} - \frac{N_1}{E_1A_1} + h \cdot \theta(x),_x \right) \\ N_{1,xx} - k_s N_1 \left[ \frac{1}{E_2A_2} + \frac{1}{E_1A_1} \right] &= -k_s \cdot \left( \frac{F}{E_2A_2} + h \cdot \theta(x),_x \right) \\ N_{1,xx} - k_s N_1 \left[ \frac{1}{E_2A_2} + \frac{1}{E_1A_1} \right] &= -k_s \cdot \left( \frac{F}{E_2A_2} - h \cdot \frac{M+N_1h-Fy_2}{E_1I_1+E_2I_2} \right) \\ N_{1,xx} - k_s N_1 \left[ \frac{1}{E_2A_2} + \frac{1}{E_1A_1} + \frac{h^2}{E_1I_1+E_2I_2} \right] &= -k_s \cdot \left( \left( \frac{1}{E_2A_2} + \frac{hy_2}{E_1I_1+E_2I_2} \right) F - \frac{Mh}{E_1I_1+E_2I_2} \right) \\ N_{1,xx} - \alpha^2 N_1 &= \frac{k_s h}{E_1I_1+E_2I_2} \cdot M - k_s \left( \frac{1}{E_2A_2} + \frac{hy_2}{E_1I_1+E_2I_2} \right) F \\ \frac{d^2 N_1}{dx^2} - \alpha^2 N_1 &= \frac{k_s h}{\sum E_i I_i} M - k_s \left( \frac{1}{E_2A_2} + \frac{hy_2}{\sum E_i I_i} \right) F \end{aligned} \quad (13)$$

with

$$\begin{aligned}
 \theta(x)_{,x} &= -\frac{M_1}{E_1 I_1} = -\frac{M_2}{E_2 I_2} = -\frac{M+N_1 h-F y_2}{E_1 I_1+E_2 I_2} \\
 M_1 &= -E_1 I_1 \cdot \theta(x)_{,x} \\
 M_2 &= -E_2 I_2 \cdot \theta(x)_{,x} \\
 M &= M_1 + M_2 - N_1 h + F y_2 = -(E_1 I_1 + E_2 I_2) \theta(x)_{,x} - N_1 h + F \\
 \sum E_i I_i &= E_1 I_1 + E_2 I_2
 \end{aligned} \tag{14}$$

where  $\alpha$  is the connector shear parameter.

$$\alpha^2 = k_s \left[ \frac{1}{E_2 A_2} + \frac{1}{E_1 A_1} + \frac{h^2}{E_1 I_1 + E_2 I_2} \right] = k_s \left( \frac{1}{E_2 A_2} + \frac{1}{E_2 A_2} + \frac{h^2}{\sum E_i I_i} \right) \tag{15}$$

## Dynamic analysis using shear deformation theories

### *Timoshenko's first-order shear deformation theory*

Consider a mixed beam that is composed of two elements. According to the Timoshenko hypothesis, there is a uniform shear and deformations due to transverse shear should not be neglected, which requires the introduction of a shear correction factor. In this case, the displacement field may be written in the following form:

$$\begin{cases} u_1(x, z) = u_{01} + z\theta(x) \\ u_2(x, z) = u_{02} + z\theta(x) \\ w(x, z) = w_0 \end{cases} \tag{16}$$

where  $u_{01}$ ,  $u_{02}$  and  $w_0$  are unknown displacements of the midplane of each element of the beam, and  $f(z)$  represents a shape function that describes the variation of transverse shear stresses and that of stresses through the beam thickness. The deformation relations are given by:

$$\begin{cases} \varepsilon_{xx1} = \frac{\partial u_1(x, z)}{\partial x} = u_{01,x} + z\theta_{,x} \\ \varepsilon_{xx2} = \frac{\partial u_2(x, z)}{\partial x} = u_{02,x} + z\theta_{,x} \\ \gamma_{xz1} = \gamma_{xz2} = \frac{\partial u_1(x, z)}{\partial z} + \frac{\partial w(x, z)}{\partial x} = \theta + w_{,x} \end{cases} \tag{17}$$

### Equations of motion

The equations of motion are obtained using Hamilton's principle which is expressed as follows:

$$\int_{t_1}^{t_2} ((\delta T - \delta U - \delta U_s)) dt = 0 \quad (18)$$

Here  $\delta U$  is the variation of the virtual strain energy,  $\delta U_s$  is the variation of the strain energy of the connectors, and  $\delta T$  is the variation of the total kinetic energy.

The deformation energy of the beam is given by the following relation:

$$U = \frac{1}{2} \iiint (\sigma_{1xx} \cdot \varepsilon_{1xx} + \sigma_{2xx} \cdot \varepsilon_{2xx} + \tau_{1xz} \cdot \gamma_{1xz} + \tau_{2xz} \cdot \gamma_{2xz}) dx dy dz = 0 \quad (19)$$

$$U = \frac{1}{2} \iiint (E_1 (\varepsilon_{1xx})^2 + E_2 (\varepsilon_{2xx})^2 + G_1 (\gamma_{1xz})^2 + G_2 (\gamma_{2xz})^2) dx dy dz = 0 \quad (20)$$

with

$$\begin{aligned} \sigma_{xx} &= E \cdot \varepsilon_{xx} \quad \text{et} \quad \tau_{xz} = G \gamma_{xz} \\ U &= \frac{1}{2} \iiint \left( (E_1 (u_{01,x} + z \theta_{,x})^2 + E_2 (u_{02,x} + z \theta_{,x})^2 \right. \\ &\quad \left. + G_1 (w_{,x} + \theta)^2 + G_2 (w_{,x} + \theta)^2) \right) dx dy dz \end{aligned} \quad (21)$$

Hence, minimization of the strain energy allows writing:

$$\begin{aligned} \delta U &= - \int (E_1 A_1 \delta u_{01,x} \cdot u_{01,x} + E_1 I_1 \cdot \theta_{,x} \cdot \delta \theta_{,x}) dx \\ &\quad - \int (E_2 A_2 \cdot u_{02,x} \delta u_{02,x} + E_2 I_2 \cdot \theta_{,x} \cdot \delta \theta_{,x}) dx \\ &\quad + \int KGA^1 (\theta + w_{,x}) (\delta \theta + \delta w_{,x}) dx \\ &\quad + \int KGA^2 (\theta + w_{,x}) (\delta \theta + \delta w_{,x}) dx \end{aligned} \quad (22)$$

with

$$\begin{aligned} \iint E_1 dy dz &= E_1 A_1, \quad \iint E_2 dy dz = E_2 A_2, \quad \iint E_1 z^2 dy dz = E_1 I_1, \\ \iint E_2 z^2 dy dz &= E_2 I_2 \end{aligned} \quad (23)$$

where  $K$  is a shear correction factor used for transverse shear stress correction. The deformation energy due to the interlaminar sliding of the layers of the composite beam is given by the following relation (Type I slip field):

$$U_s = \frac{I}{2} \int K_s(u_{02}-u_{01}-h\theta)^2 dx \quad (24)$$

After minimization, the following expression is then obtained:

$$\delta U_s = \int K_s(u_{02}-u_{01}-h\theta)(\delta u_{02}-\delta u_{01}-h\delta\theta)dx \quad (25)$$

The kinetic energy of the composite beam under study is then given as:

$$T = \frac{I}{2} \int m \dot{w}^2 dx = \frac{I}{2} \int (m_1+m_2) \dot{w}^2 dx \quad (26)$$

After minimization, the kinetic energy then becomes:

$$\delta T = \int (m_1+m_2) \dot{w} \delta \dot{w} dx \quad (27)$$

Subsequently, substituting equations 22, 25 and 27 into equation (18) gives the following equilibrium equations:

$$\begin{aligned} & \iiint (\delta T - \delta U - \delta U_s) dt = \iiint (m_1+m_2) w \delta \dot{w} dx dt \\ & - \int (E_1 A_1 \delta u_{01,x} \cdot u_{01,x} + E_1 I_1 \cdot \theta_{,x} \cdot \delta \theta_{,x}) dx dy \\ & - \int (E_2 A_2 \cdot u_{02,x} \delta u_{02,x} + E_2 I_2 \cdot \theta_{,x} \delta \theta_{,x}) dx dy \\ & + \int K G A^1 (\theta + w_{,x}) (\delta \theta + \delta w_{,x}) dx dt \\ & + \int K G A^2 (\theta + w_{,x}) (\delta \theta + \delta w_{,x}) dx dt \\ & - \int K_s (u_{02}-u_{01}-h\theta) (\delta u_{02}-\delta u_{01}-h\delta\theta) dx dt \end{aligned} \quad (28)$$

Afterwards, integration by part allows obtaining the system of differential equations describing the free vibration motion of a mixed Timoshenko beam:

$$\begin{aligned} eq1 &= E_2 A_2 \left( \frac{\partial^2}{\partial x^2} u_{02}(x) \right) - K_s (u_{02}(x) - u_{01}(x) + h\theta(x)) \\ eq2 &= E_1 A_1 \left( \frac{\partial^2}{\partial x^2} u_{01}(x) \right) + K_s (u_{02}(x) - u_{01}(x) + h\theta(x)) \\ eq3 &= (E_1 I_1 + E_2 I_2) \left( \frac{\partial^2}{\partial x^2} \theta(x) \right) - (K_1 G_1 A_1 + K_2 G_2 A_2) \left( \frac{\partial}{\partial x} w(x,t) + \theta(x) \right) \end{aligned} \quad (29)$$

$$+K_S h (u_{02}(x)-u_{01}(x)+h\theta(x))$$

$$eq 4 = (K_1 G_1 A_1 + K_2 G_2 A_2) \left( \frac{\partial^2}{\partial x^2} w(x,t) + \frac{\partial}{\partial x} \theta(x) \right) - m \omega^2 w(x,t)$$

### High order shear deformation theory

Unlike the classical theory and the Timoshenko theory, which are both based on the linear distribution of displacement through the beam thickness, the high order theory is based on a nonlinear distribution of fields through the thickness. For this reason, it was deemed necessary to take into account the effects of the transverse shear strain and the transverse normal strain. It should be noted that the models considered do not require a correction factor. This theory is more precise than the first order theory as it introduces a function that takes into account the warping phenomenon. The present study takes into account the warping effect which uses a new transverse deformation function and can be written in the following form:

$$\begin{cases} U_1(x,z,t) = u_1(x,t) - z \frac{\partial}{\partial x} w(x,t) + f(z) \cdot \theta_1(x,t) \\ U_2(x,z,t) = u_2(x,t) - z \frac{\partial}{\partial x} w(x,t) + f(z) \cdot \theta_2(x,t) \\ W(x,z,t) = w(x,t) \end{cases} \quad (30)$$

Substituting the strain energy into equation (19) gives:

$$U = \frac{1}{2} \left( \int_{\frac{h_1}{2}}^{\frac{h_1}{2}} E_1 b_1 \left( \frac{\partial U_1(x,z,t)}{\partial x} \right)^2 dz + \int_{\frac{h_2}{2}}^{\frac{h_2}{2}} E_2 b_2 \left( \frac{\partial U_2(x,z,t)}{\partial x} \right)^2 dz + \int_{\frac{h_1}{2}}^{\frac{h_1}{2}} K_1 G_1 b_1 \left( \frac{\partial U_1(x,z,t)}{\partial z} \right)^2 dz + \int_{\frac{h_2}{2}}^{\frac{h_2}{2}} K_2 G_2 b_2 \left( \frac{\partial U_2(x,z,t)}{\partial z} \right)^2 dz \right) dx \quad (31)$$

$$U = \frac{1}{2} \left( \int_{\frac{h_1}{2}}^{\frac{h_1}{2}} E_1 b_1 \left( \frac{\partial}{\partial x} u_1(x,t) - z \frac{\partial^2}{\partial x^2} w(x,t) + f(z) \frac{\partial}{\partial x} \theta_1(x,t) \right)^2 dz + \int_{\frac{h_2}{2}}^{\frac{h_2}{2}} E_2 b_2 \left( \frac{\partial}{\partial x} u_2(x,t) - z \frac{\partial^2}{\partial x^2} w(x,t) + f(z) \frac{\partial}{\partial x} \theta_2(x,t) \right)^2 dz \right) \quad (32)$$

$$\begin{aligned}
& + \int_{\frac{h_1}{2}}^{\frac{h_1}{2}} k_1 b_1 G_1 \left( -\frac{\partial}{\partial x} w(x,t) + \left( \frac{d}{dz} f(z) \right) \theta_1(x,t) \right)^2 dz \\
& + \int_{\frac{h_2}{2}}^{\frac{h_2}{2}} k_2 b_2 G_2 \left( -\frac{\partial}{\partial x} w(x,t) + \left( \frac{d}{dz} f(z) \right) \theta_2(x,t) \right)^2 dz \Big) dx
\end{aligned}$$

The present theory is based on a new interlaminar slip field that was initially developed by N. Elmeiche, I. Mechab, and F. Bernard. This field takes into account the longitudinal sliding of the two elements of the composite beam, the rotating sliding, and the sliding that is due to the transverse warping of the beam (new type II slip field):

$$\begin{aligned}
U_s = & \int \frac{1}{2} k_s \left( u_2(x) - u_1(x) - \frac{h_1}{2} \cdot \theta_1(x) - \frac{h_2}{2} \cdot \theta_2(x) \right. \\
& \left. - \left( f(z) \Big|_{z=\frac{h_1}{2}} \right) \cdot \left( \frac{\partial W(x,z,t)}{\partial x} + \theta_1(x) \right) \right. \\
& \left. - \left( f(z) \Big|_{z=\frac{h_2}{2}} \right) \cdot \left( \frac{\partial W(x,z,t)}{\partial x} + \theta_2(x) \right) \right)^2 dx
\end{aligned} \tag{33}$$

In addition, the kinetic energy along the three directions, with the rotational inertia (RT), can be expressed in the form:

$$\begin{aligned}
T = & \frac{1}{2} \int \left( \omega^2 \cdot \left( b_1 \cdot \rho_1 \cdot (U_1(x,z,t))^2 \right. \right. \\
& \left. \left. + \left( b_2 \cdot \rho_2 \cdot (U_2(x,z,t))^2 + (b_1 \cdot \rho_1 + b_2 \cdot \rho_2) \cdot (W(x,z,t))^2 \right) \right) dz \right) dx
\end{aligned} \tag{34}$$

$$\begin{aligned}
T = & \frac{1}{2} \int \left( \omega^2 b_1 u_1(x,t)^2 \left( \int \rho_1 dz \right) - \omega^2 b_1 u_1(x,t) \left( \frac{\partial}{\partial x} w(x,t) \right) \left( \int \rho_1 z dz \right) \right. \\
& \left. + \omega^2 b_1 u_1(x,t) \theta_1(x,t) \int \rho_1 f(z) dz \right. \\
& \left. + \frac{1}{2} \omega^2 b_1 \left( \frac{\partial}{\partial x} w(x,t) \right)^2 \left( \int \rho_1 z^2 dz \right) b_1 \left( \frac{\partial}{\partial x} w(x,t) \right) \theta_1(x,t) \left( \int \rho_1 z f(z) dz \right) \right. \\
& \left. + \frac{1}{2} \omega^2 b_1 \theta_1(x,t)^2 \left( \int \rho_1 f(z)^2 dz \right) + \frac{1}{2} b_2 u_2(x,t)^2 \left( \int \rho_2 dz \right) \right. \\
& \left. - \omega^2 b_2 u_2(x,t) \left( \frac{\partial}{\partial x} w(x,t) \right) \left( \int \rho_2 z dz \right) + b_2 u_2(x,t) \theta_2(x,t) \left( \int \rho_2 f(z) dz \right) \right. \\
& \left. + \frac{1}{2} \omega^2 b_2 \left( \frac{\partial}{\partial x} w(x,t) \right)^2 \left( \int \rho_2 z^2 dz \right) \right)
\end{aligned} \tag{35}$$

$$-b_2 \left( \frac{\partial}{\partial x} w(x,t) \right) \theta_2(x,t) \left( \int \rho_2 z f(z) dz \right) + \frac{1}{2} \omega^2 b_2 \theta_2(x,t)^2 \left( \int \rho_2 f(z)^2 dz \right) + \frac{1}{2} b_1 w(x,t)^2 \left( \int \rho_1 dz \right) + \frac{1}{2} \omega^2 b_2 w(x,t)^2 \left( \int \rho_2 dz \right) dx$$

with

$$\left\{ \begin{array}{l} I_{11}, I_{21}, I_{31} = \int_{-\frac{h1}{2}}^{\frac{h1}{2}} \{l, z, z^2\} \rho_1 dz \\ I_{12}, I_{22}, I_{32} = \int_{-\frac{h2}{2}}^{\frac{h2}{2}} \{l, z, z^2\} \rho_2 dz \\ I_{41}, I_{51}, I_{61} = \int_{-\frac{h1}{2}}^{\frac{h1}{2}} \{l, z, z^2\} \rho_1 \cdot f(z) dz \\ I_{42}, I_{52}, I_{62} = \int_{-\frac{h2}{2}}^{\frac{h2}{2}} \{l, z, f(z)\} \rho_2 \cdot f(z) dz \end{array} \right. \quad (36)$$

The new warping shape function, previously developed by N. Elmeiche and I. Mechab, gives:

$$f(z) = z + \frac{1}{6} \frac{z^3}{\left( \cos\left(\frac{l}{2}\right) - 1 \right) H^2} \quad (37)$$

### Static analysis using shear deformation theories

The composite beam is subjected to a uniformly distributed bending load. The work of the external force is then given as:

$$E_{we} = \frac{1}{2} \int q \cdot (W(x, z, t))^2 dx \quad (38)$$

Using the displacement field expressed in equation 30 allows writing the total energy of the composite beam as:

$$Eq = E_{we} - U - U_s = \frac{1}{2} \left( \int_{-\frac{h1}{2}}^{\frac{h1}{2}} E_1 b_1 \left( \frac{\partial}{\partial x} u_1(x, t) - z \frac{\partial^2}{\partial x^2} w(x, t) + f(z) \frac{\partial}{\partial x} \theta_1(x, t) \right)^2 dz \right. \quad (39)$$

$$\begin{aligned}
& + \int_{-\frac{h_2}{2}}^{\frac{h_2}{2}} E_2 b_2 \left( \frac{\partial}{\partial x} u_2(x,t) - z \frac{\partial^2}{\partial x^2} w(x,t) + f(z) \frac{\partial}{\partial x} \theta_2(x,t) \right)^2 dz \\
& + \int_{-\frac{h_1}{2}}^{\frac{h_1}{2}} k_1 b_1 G_1 \left( -\frac{\partial}{\partial x} w(x,t) + \left( \frac{d}{dz} f(z) \right) \theta_1(x,t) \right)^2 dz \\
& + \int_{-\frac{h_2}{2}}^{\frac{h_2}{2}} k_2 b_2 G_2 \left( -\frac{\partial}{\partial x} w(x,t) + \left( \frac{d}{dz} f(z) \right) \theta_2(x,t) \right)^2 dz \Bigg) dx \\
& + \frac{I}{2} \int k_s \left( u_2(x) - u_1(x) - \frac{h_1}{2} \cdot \theta_1(x) - \frac{h_2}{2} \cdot \theta_2(x) - \left( f(z) \Big|_{z=\frac{h_1}{2}} \right) \right. \\
& \cdot \left( \frac{\partial W(x,z,t)}{\partial x} + \theta_1(x) \right) - \left( f(z) \Big|_{z=\frac{h_2}{2}} \right) \cdot \left. \left( \frac{\partial W(x,z,t)}{\partial x} + \theta_2(x) \right) \right)^2 dx \\
& + \frac{I}{2} \int q(W(x,z,t))^2 dx
\end{aligned}$$

### Numerical solution by the Ritz method

Consider a simply supported composite beam of the length L. The numerical resolution of the problem, using the Ritz method, consists of minimizing the total energy related to the amplitudes of the displacement and rotation fields:

$$\begin{cases} u_1(x) = \sum_{i=0}^n \left[ U_{1i} \cdot \left( \frac{x}{L} \right)^i \cdot \left( \frac{x}{L} - 1 \right) \right] \\ u_2(x) = \sum_{i=0}^n \left[ U_{2i} \cdot \left( \frac{x}{L} \right)^i \cdot \left( \frac{x}{L} - 1 \right) \right] \\ \theta_1(x) = \sum_{i=0}^n \left[ \theta_{1i} \cdot \left( \frac{x}{L} \right)^i \cdot \left( \frac{x}{L} - 1 \right) \right] \\ \theta_2(x) = \sum_{i=0}^n \left[ \theta_{2i} \cdot \left( \frac{x}{L} \right)^i \cdot \left( \frac{x}{L} - 1 \right) \right] \\ w(x) = \sum_{i=0}^n \left[ W_i \cdot \left( \frac{x}{L} \right)^i \cdot \left( \frac{x}{L} - 1 \right) \right] \end{cases} \quad (40)$$



After the substitution and the minimization of the Ritz solutions in equations 32 - 36, a square matrix of the dimension  $5.(n+1).5.(n+1)$  may then be obtained in the following form (see Appendix):

$$\begin{pmatrix} [A_{11}][A_{12}][A_{13}][A_{14}][A_{15}]_i \\ [A_{21}][A_{22}][A_{23}][A_{24}][A_{25}]_i \\ [A_{31}][A_{32}][A_{33}][A_{34}][A_{35}]_i \\ [A_{41}][A_{42}][A_{43}][A_{44}][A_{45}]_i \\ [A_{51}][A_{52}][A_{53}][A_{54}][A_{55}]_i \end{pmatrix}_{i=0..n} \cdot \begin{Bmatrix} \{U_{1i}\} \\ \{U_{2i}\} \\ \{\theta_{1i}\} \\ \{\theta_{2i}\} \\ \{W_i\} \end{Bmatrix}_{i=0..n} = \begin{Bmatrix} \{0_i\} \\ \{0_i\} \\ \{0_i\} \\ \{0_i\} \\ \{0_i\} \end{Bmatrix}_{i=0..n} \quad (41)$$

In dynamics, the determinant of the system of equations gives the natural vibration frequencies:

$$\omega^2 = \det[A] \quad (42)$$

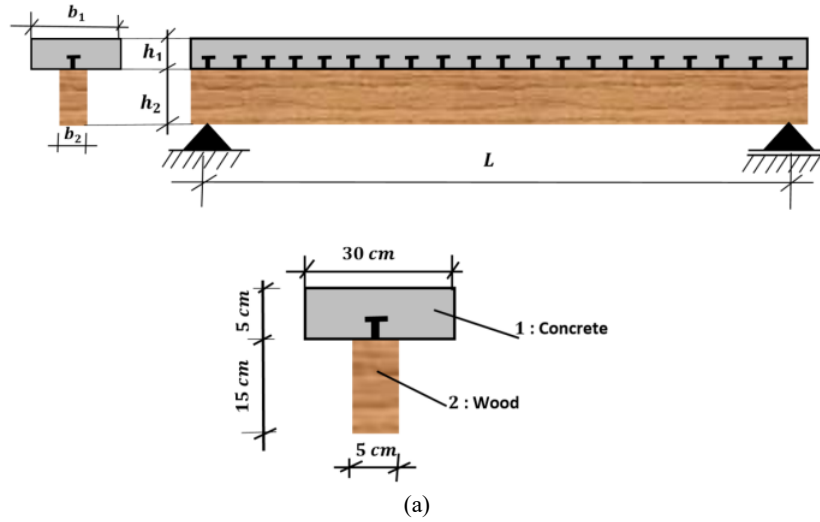
### Digital application

The numerical calculation of the natural frequency of vibration and the interlaminar shear force of two types of simply supported composite beams with a partial connection between the materials was carried out. The first composite beam is made of concrete-wood materials, with a T-shaped cross section. It is composed of a concrete slab, rectangular in shape in its upper part, while the lower part is made of wood.

The other composite beam has an I-shaped cross section. It is made of a concrete slab, rectangular in shape in its upper part, while the lower part has a HEA steel profile in the form of the capital letter I. The properties of each composite beam are presented in Figure 5.

Furthermore, a validation study of the ten free vibration frequencies was carried out using the first order shear deformation theory of the composite beam made of concrete-wood materials. The results, depicted in Table 1, were verified and then compared with those reported in the work of Xu & Wu (2008). In this study, a shear correction factor equal to  $5/6$  was used. The relative frequency error, for all modes, did not exceed 0.37%, which means that the frequency values found in the present work are in good agreement with those reported in the literature.

$E_1=12\text{GPa}$ ,  $E_2=8\text{GPa}$ ,  $G_1=5\text{GPa}$ ,  $G_2=3\text{GPa}$ ,  $m_1=34.5\text{kg}$ ,  $m_2=5.25\text{kg}$ ,  $K_{sc}=50\text{MPa}$



<b>HEA 200 SIS 1312</b>	$b_1=1.5\text{ m}$	$r=0.145\text{ m}$	$K=0.20$	$E_1 I_1=1.06$	$\alpha=0.901\text{ m}^{-1}$
$A_2=5.383 \times 10^{-3}\text{ m}^2$	$b_2=0.2\text{ m}$	$r_1=0.050\text{ m}$	$E_1=8.5^\circ$	$E_2 I_2=7.75$	$El_0/El_\infty=0.412$
$I_2=3.692 \times 10^{-5}\text{ m}^2$	$h_1=0.10\text{ m}$	$r_2=0.095\text{ m}$	$E_2=210$	$El_0=8.81$	$\alpha L=5.40\text{ for }L=6\text{ m}$
$t_{\text{flange}}=0.010\text{ m}$	$h_2=0.19\text{ m}$	$z_{cg, \infty}=0.0681\text{ m}$	$E_1 A_1=1275$	$El_\infty=21.4$	
$t_{\text{web}}=0.0065\text{ m}$			$E_2 A_2=1130$	$El_{\text{eff}}=15.7\text{ for }L=6\text{ m}$	
			$EA_0=2405$	And $\mu=1$	

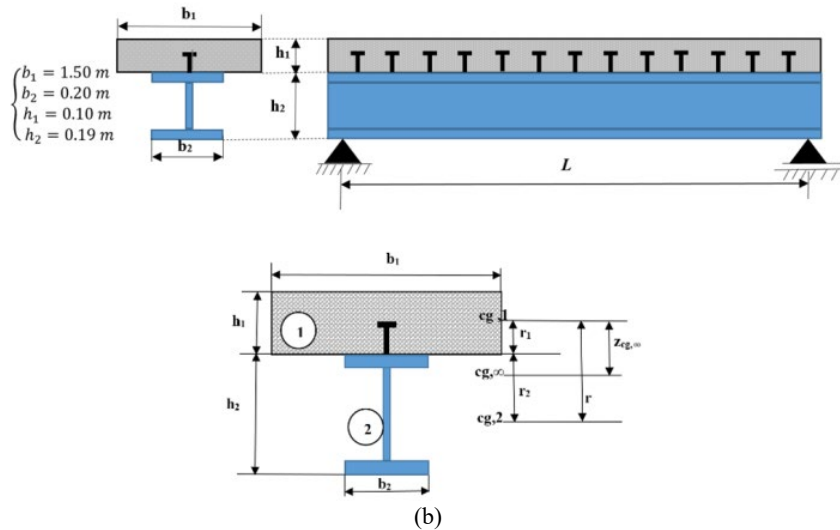


Figure 5 – Types of the beams under study:(a) Mixed beam in concrete-wood materials (materials I);(b) composite beam in steel-concrete materials (materials II)

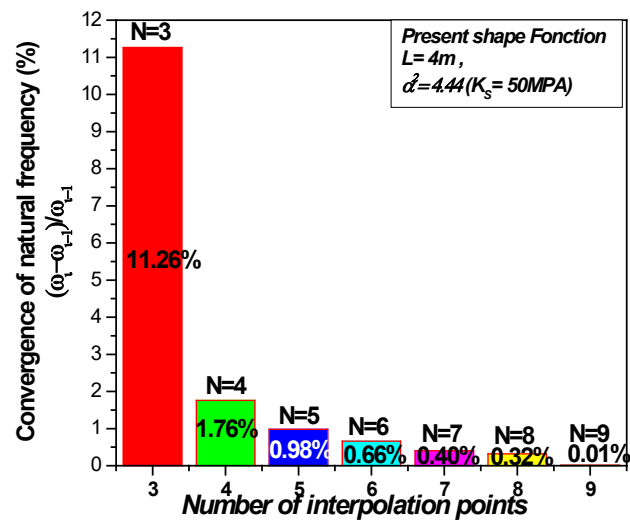


Figure 6 – Convergence test of the vibration frequency for the composite beam I

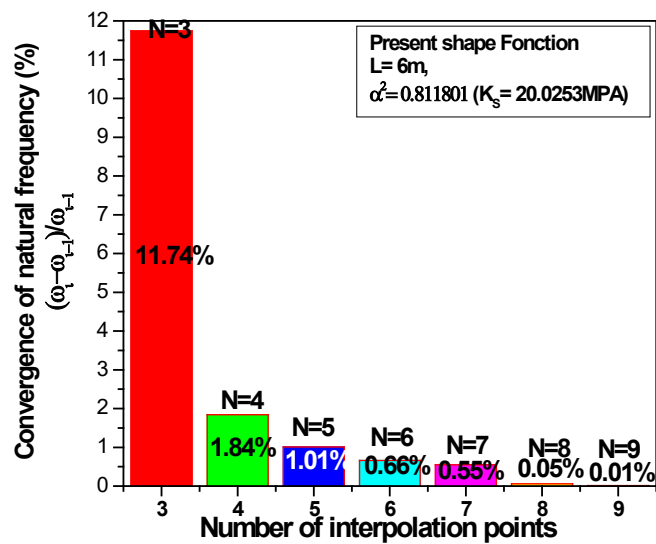


Figure 7 – Convergence test of the vibration frequency for the composite beam II

Table 1 – First ten vibration frequencies (Hz) of the composite beam made of material I with a sliding field of type I

L/H	Mode	Present	Xu & Wu (2008)		Relative error %
			Exact	DQM	
20	1	10.2787	10.2768	10.3023	0.02
	2	33.1627	33.1771	33.3569	0.04
	3	65.2411	65.3343	65.8811	0.14
	4	107.0528	107.3095	108.6140	0.24
	5	158.6972	159.2021	161.9071	0.32
	6	219.8142	220.6233	225.6710	0.37
	7	289.8239	290.9092	299.5853	0.37
	8	368.0599	369.2557	383.2073	0.32
	9	453.8387	454.7913	476.0263	0.21
	10	546.5014	546.6124	577.4941	0.02

Table 2 – Natural frequency of the composite beam made of concrete and wood materials as a function of the shear parameter  $\alpha^2$  of the connectors, with shear deformation (SD) and rotary inertia (RI), for a type II slip field

Number of interpolation N=9, Present with (SD and RI)								
L/H=5					L/H=10			
Theories	PSDBT	HSDBT	Present	Error	PSDBT	HSDBT	Present	Error
$\alpha^2$								
$10^{-3}$	79.159	80.461	81.070	0.76%	39.330	39.939	40.248	0.77%
$10^{-2}$	79.186	80.489	81.097	0.76%	39.344	39.953	40.261	0.77%
$10^{-1}$	79.462	80.760	81.363	0.75%	39.484	40.090	40.395	0.76%
1	82.095	83.390	83.906	0.62%	40.752	41.336	41.607	0.66%
10	101.394	102.504	102.664	0.16%	48.564	49.025	48.885	0.29%
50	140.572	141.081	141.127	0.03%	58.094	58.404	58.656	0.43%
$10^2$	160.831	160.992	161.128	0.08%	61.399	61.667	61.877	0.34%
$5.5.10^2$	194.117	194.142	194.099	0.02%	65.130	65.349	65.549	0.31%
$10^3$	199.265	199.229	199.203	0.01%	65.575	65.790	65.989	0.30%
$5.5.10^3$	205.015	204.911	204.193	0.35%	66.041	66.253	66.455	0.30%
$10^4$	205.676	205.559	205.57	0.01%	66.094	66.304	66.506	0.30%
Number of interpolation N=9, Present with (SD and RI)								
L/H=15					L/H=20			

Theories	PSDBT	HSDBT	Present	Error	PSDBT	HSDBT	Present	Error
$\alpha^2$								
$10^{-3}$	25.887	26.516	26.757	0.91%	19.499	19.884	20.010	0.63%
$10^{-2}$	25.897	26.526	26.766	0.90%	19.506	19.890	20.016	0.63%
$10^{-1}$	25.994	26.615	26.854	0.90%	19.574	19.957	20.082	0.63%
1	26.811	27.377	27.603	0.83%	20.109	20.483	20.597	0.56%
10	30.670	31.056	31.240	0.59%	22.227	22.539	22.641	0.45%
50	34.142	34.410	34.595	0.54%	23.707	23.948	24.089	0.59%
$10^2$	35.002	35.248	35.440	0.54%	24.029	24.254	24.410	0.64%
$5.5 \cdot 10^2$	35.867	36.091	36.291	0.55%	24.341	24.549	24.718	0.69%
$10^3$	35.961	36.185	36.385	0.55%	24.374	24.582	24.751	0.69%
$10^{-3}$	36.060	36.292	36.482	0.52%	24.408	24.616	24.785	0.69%

Table 3 – Natural frequency of the composite beam made of concrete and steel materials as a function of the shear parameter  $\alpha^2$  of the connectors, with shear deformation (SD) and rotary inertia (RI), for a type II slip field

Number of interpolation N=9, Present with (SD and RI)

L/H=5

L/H=10

Theories	PSDBT	HSDBT	Present	Error	PSDBT	HSDBT	Present	Error
$\alpha^2$								
$10^{-3}$	29.468	29.956	30.153	0.66%	13.804	14.103	14.124	0.15%
$10^{-2}$	29.589	30.075	30.271	0.65%	13.868	14.167	14.186	0.13%
$10^{-1}$	30.772	31.234	31.420	0.60%	14.484	14.786	14.784	0.01%
1	40.241	40.566	40.686	0.30%	19.982	19.304	19.182	0.63%
10	79.833	80.132	79.876	0.32%	33.475	33.485	33.305	0.54%
50	122.680	123.310	122.502	0.66%	42.668	42.665	42.644	0.05%
$10^2$	136.870	136.326	136.530	0.15%	44.629	44.616	44.596	0.04%
$5.5 \cdot 10^2$	153.651	153.362	153.268	0.06%	46.496	46.478	46.454	0.05%
$10^3$	155.769	155.467	155.370	0.06%	46.706	46.691	46.661	0.06%
$5.5 \cdot 10^3$	158.435	157.983	158.739	0.48%	46.989	46.962	46.895	0.14%
$10^4$	159.121	158.748	159.133	0.24%	47.065	47.029	47.027	0.00%

Number of interpolation N=9, Present with (SD and RI)

L/H=15

L/H=20

Theories	PSDBT	HSDBT	Present	Error	PSDBT	HSDBT	Present	Error
$\alpha^2$								
$10^{-3}$	9.029	9.179	9.235	0.61%	6.715	6.839	6.870	0.45%
$10^{-2}$	9.073	9.222	9.277	0.60%	6.748	6.871	6.902	0.45%
$10^{-1}$	9.481	9.623	9.675	0.54%	7.048	7.167	7.195	0.39%
1	12.214	12.324	12.348	0.19%	8.889	8.990	9.000	0.11%
10	19.039	19.110	19.083	0.14%	12.469	12.582	12.557	0.20%
50	21.898	21.921	21.919	0.01%	13.587	13.620	13.645	0.18%
$10^2$	22.391	22.417	22.408	0.04%	13.756	13.791	13.809	0.13%
$5.5 \cdot 10^2$	22.829	22.851	22.881	0.13%	13.903	13.939	13.951	0.09%
$10^3$	22.867	22.887	22.914	0.12%	13.919	13.955	13.967	0.09%
$5.5 \cdot 10^3$	22.936	22.959	22.968	0.04%	13.939	13.977	13.987	0.07%
$10^{-3}$	22.952	23.010	22.984	0.11%	13.944	13.956	13.992	0.26%

Tables 2 and 3 present the variation of the natural vibration frequencies of the composite beam in concrete-wood and concrete-steel materials as a function of the shear parameter of the connectors with transverse shear deformation (SD) and rotational inertia (RI). The results of the present theory with a new warping shape function (equation 37) were then recorded and compared with those given by the parabolic shear strain beam theory (PSDBT) and the hyperbolic shear strain beam theory (HSDBT). For the different slenderness values of the two types of beams, the relative error did not exceed 0.91% for the beam in material I and 0.66% for the beam in material II. The results obtained for the two types of beams are in good agreement. This is certainly due to the perfect convergence of the Ritz method and the new shear strain function.

The dynamic analysis of the natural frequency of vibrations with transverse shear deformation (SD) and rotational inertia (RI) of the composite beam made of concrete-wood materials and concrete-steel materials is presented in Figures 8 and 9. The values of the connector shear parameter  $\alpha^2$  are given by a logarithmic scale with the new interlaminar slip field (type II slip field). The frequency is stationary for low connector parameter values, i.e.,  $\alpha^2$  between  $10^{-3}$  and  $10^{-1}$ . This frequency gradually increases while exhibiting a non-linear behavior, and the deviation point of the curves is observed at  $\alpha^2 = 10$ . In addition, the difference between the maximum frequency, which corresponds to  $\alpha^2 = 10^4$ , and the frequency that corresponds to  $\alpha^2 = 10$  and which is considered

as the point of deviation of the curves, varies from 55.33% to 1.42% for type I material and from 52.46% to 8.24% for type II material. The maximum deviation is obtained with the short composite beam ( $L/H = 5$ ) and the minimum deviation is observed with the slender composite beam ( $L/H = 20$ ). The nonlinear behavior of the beam is due to the fact that the significant effects of transverse shear and warping of the short composite beam, for type I and II materials, are taken into account.

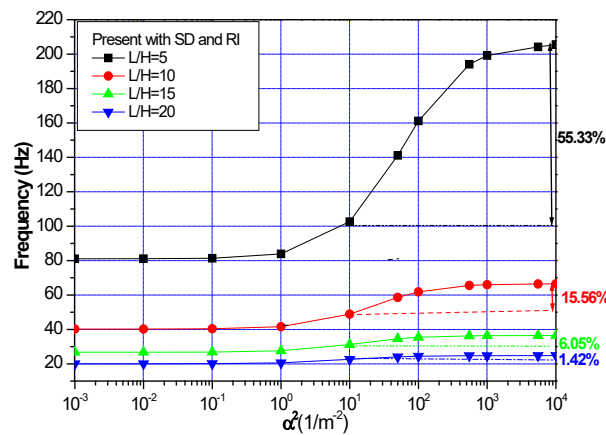


Figure 8 – Variation of the natural frequency of the composite beam made of concrete and wood materials as a function of the shear parameter  $\alpha^2$  of the connectors, for a type II slip field

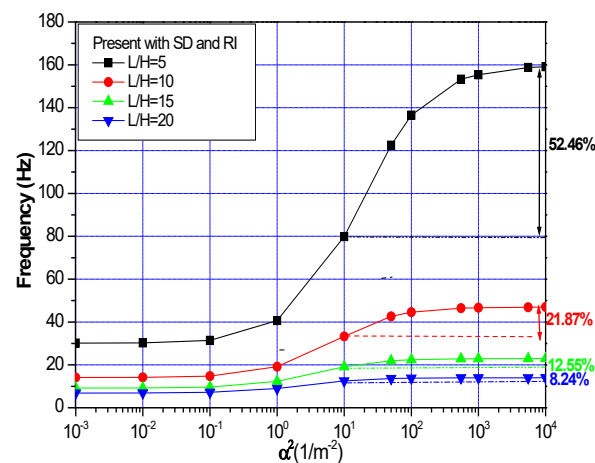


Figure 9 – Variation of the natural frequency of the composite beam made of concrete and steel materials as a function of the shear parameter  $\alpha^2$  of the connectors, for a type II slip field

### Analysis of bending

The static analysis is based on the numerical calculation of the bending of the two composite beams made with materials I and II. The two beams are simply supported and are subjected to a uniformly distributed load, with  $q = 15 \text{ KN/m}$  and  $q = 4 \text{ KN/m}$ , respectively. Figures 9 and 10 illustrate the variation of the interlaminar shear force as a function of the shear coefficient of the connectors.

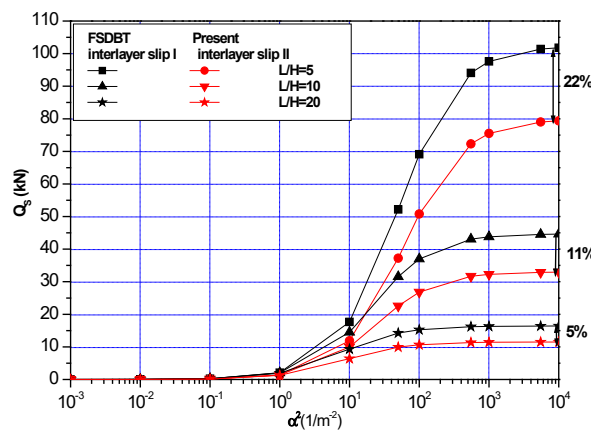


Figure 10 – Variation of the interlaminar shear force  $Q_s$  for the composite beam made of steel-concrete materials

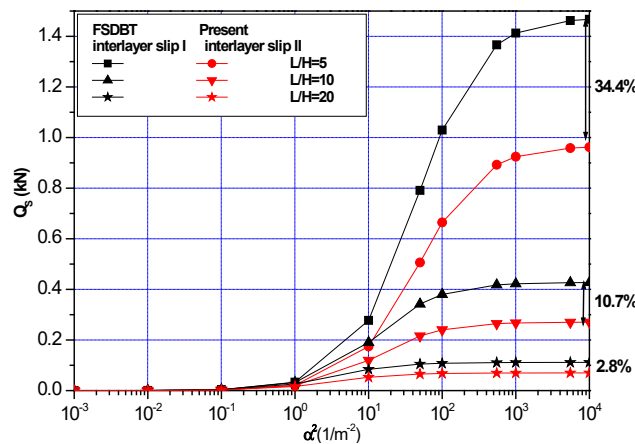


Figure 11 – Variation of the interlaminar shear force  $Q_s$  for the composite beam made of concrete-wood materials



Figures 10 and 11 show the variation of the interlaminar shear force for the two materials I and II, with two interlaminar slip fields, i.e., a classic sliding field of the Timoshenko beam, and a new sliding field proposed using the higher order theory. The deviation of the interlaminar shear force, for the two slip fields, varies from 22% to 11%, and to 5%, respectively, for the beams of material I with the slenderness ( $L/H$ ) equal to 5, 10 and 20. The deviation of the interlaminar shear force for the two slip fields varies from 34% to 10.7% and to 2.8%, respectively, for the beams of material II with the slenderness ( $L/H$ ) equal to 5, 10 and 20. These findings suggest that the introduction of the warping effect into the new interlaminar slip field of a composite beam is significantly important, which is not the case for the slender beam because in this case the transverse shear and the warping effects are negligible. Based on the above, it can be said that the composite beam behaves like an Euler-Bernoulli beam.

## Conclusion

The present study primarily focused on the detailed investigation of the dynamic part and the static part of a composite beam that was analyzed using different theories. A new interlaminar slip field of a composite beam was then introduced in the method used. This field accounts for the warping effect with a new transverse shear strain shape function. The equations of motion were deduced and solved using the Ritz numerical method, while considering two different types of composite beams, i.e., a composite beam made of steel and wood materials and another made of steel and concrete materials. The numerical results obtained were compared with those found in the literature. These results were also compared with others obtained from deformation theories. It was found that the free frequency of vibration with transverse deformation shear and rotational inertia of the two composite beams in steel-wood and steel-concrete materials with a new interlaminar slip field was quite significant for the short beam but not very important for the long beam.

A similar remark was made for the static case of the interlaminar shear force. This was primarily due to the introduction of the new shear strain shape function in the equilibrium equations and in the new interlaminar slip field. These findings describe quite well the behavior of composite beams with cross-sectional warping. Furthermore, it turned out that the proposed sliding model can be employed in characterizing the real behavior of short composite beams undergoing small and large deformations.

## Appendix

$$[A] = \begin{pmatrix} [A_{11}] [A_{12}] [A_{13}] [A_{14}] [A_{15}]_i \\ [A_{21}] [A_{22}] [A_{23}] [A_{24}] [A_{25}]_i \\ [A_{31}] [A_{32}] [A_{33}] [A_{34}] [A_{35}]_i \\ [A_{41}] [A_{42}] [A_{43}] [A_{44}] [A_{45}]_i \\ [A_{51}] [A_{52}] [A_{53}] [A_{54}] [A_{55}]_i \end{pmatrix} \quad (43)$$

$$[A_{11}] = [A_{12}] = [A_{21}] = [A_{13}] = [A_{31}] = [A_{14}] = [A_{41}] = [A_{15}] = [A_{51}] = \begin{bmatrix} \frac{d}{dU1_0} E_q & \cdots & \frac{d}{dU1_0} E_q \\ \vdots & \ddots & \vdots \\ \frac{d}{dU1_i} E_q & \cdots & \frac{d}{dU1_i} E_q \end{bmatrix}_{i=0..9}$$

$$[A_{22}] = [A_{23}] = [A_{32}] = [A_{24}] = [A_{42}] = [A_{25}] = [A_{52}] = \begin{bmatrix} \frac{d}{dU2_0} E_q & \cdots & \frac{d}{dU2_0} E_q \\ \vdots & \ddots & \vdots \\ \frac{d}{dU2_i} E_q & \cdots & \frac{d}{dU2_i} E_q \end{bmatrix}_{i=0..9}$$

$$[A_{33}] = [A_{34}] = [A_{43}] = [A_{35}] = [A_{53}] = \begin{bmatrix} \frac{d}{d\theta1_0} E_q & \cdots & \frac{d}{d\theta1_0} E_q \\ \vdots & \ddots & \vdots \\ \frac{d}{d\theta1_i} E_q & \cdots & \frac{d}{d\theta1_i} E_q \end{bmatrix}_{i=0..9}$$

$$[A_{44}] = [A_{45}] = [A_{54}] = \begin{bmatrix} \frac{d}{d\theta2_0} E_q & \cdots & \frac{d}{d\theta2_0} E_q \\ \vdots & \ddots & \vdots \\ \frac{d}{d\theta2_i} E_q & \cdots & \frac{d}{d\theta2_i} E_q \end{bmatrix}_{i=0..9}$$

$$[A_{55}] = \begin{bmatrix} \frac{d}{dW_0} E_q & \cdots & \frac{d}{dW_0} E_q \\ \vdots & \ddots & \vdots \\ \frac{d}{dW_i} E_q & \cdots & \frac{d}{dW_i} E_q \end{bmatrix}_{i=0..9} \quad (44)$$

## References

- Adam, C. & Furtmüller, T. 2020. Flexural vibrations of geometrically nonlinear composite beams with interlayer slip. *Acta Mechanica*, 231, pp.251-271. Available at: <https://doi.org/10.1007/s00707-019-02528-2>.
- Barbosa, W.C.S., Bezerra, L.M., Chater, L. & Cavalcante, O.R.O. 2019. Experimental evaluation on the structural behavior of truss shear connectors in composite steel-concrete beams. *Revista IBRACON de Estruturas e Materiais*, 12(5), pp.1157-1182. Available at: <https://doi.org/10.1590/S1983-41952019000500010>.
- Carvalho, T.A., Lemes, Í.J.M., Silveira, R.A.M., Dias, L.E.S. & Barros, R.C. 2021. Concentrated Approaches for Nonlinear Analysis of Composite Beams with Partial Interaction. *ce/papers*, 4(2-4), pp.715-722. Available at: <https://doi.org/10.1002/cepa.1353>.
- Castel, A. 2013. *Comportement vibratoire de structures composites intégrant des éléments amortissants*. PhD thesis. Nevers, France: Université de Bourgogne, École doctorale Sciences pour l'ingénieur et microtechniques, Département de Recherche en Ingénierie des Véhicules pour l'Environnement (DRIVE) [online]. Available at: <https://www.sudoc.fr/177960620> [Accessed: 06 December 2024].
- Čas, B., Planinc, I. & Schnabl, S. 2018. Analytical solution of three-dimensional two-layer composite beam with interlayer slips. *Engineering Structures*, 173, pp.269-282. Available at: <https://doi.org/10.1016/j.engstruct.2018.06.108>.
- Della Croce, L. & Venini, P. 2004. Finite elements for functionally graded Reissner–Mindlin plates. *Computer Methods in Applied Mechanics and Engineering*, 193(9-11), pp.705-725. Available at: <https://doi.org/10.1016/j.cma.2003.09.014>.
- Galuppi, L. & Royer-Carfagni, G. 2014. Buckling of three-layered composite beams with viscoelastic interaction. *Composite Structures*, 107, pp.512-521. Available at: <https://doi.org/10.1016/j.compstruct.2013.08.006>.
- Honarvar, H., Shayanfar, M., Babakhani, B. & Zabihi-Samani, M. 2020. Numerical Analysis of Steel-Concrete Composite Beam with Blind Bolt under Simultaneous Flexural and Torsional Loading. *Civil Engineering Infrastructures Journal (CEIJ)*, 53(2), pp.379-393. Available at: <https://doi.org/10.22059/cej.2020.287376.1606>.
- Kant, T. & Swaminathan, K. 2001. Free vibration of isotropic, orthotropic, and multilayer plates based on higher order refined theories. *Journal of Sound and Vibration*, 241(2), pp.319-327. Available at: <https://doi.org/10.1006/jsvi.2000.3232>.
- Le Grogne, P., Nguyen, Q.-H. & Hjiat, M. 2012. Exact buckling solution for two-layer Timoshenko beams with interlayer slip. *International Journal of Solids and Structures*, 49(1), pp.143-150. Available at: <https://doi.org/10.1016/j.ijsolstr.2011.09.020>.
- Lemes, Í.J.M., Dias, L.E.S., Silveira, R.A.M., Silva, A.R. & Carvalho, T.A. 2021. Numerical analysis of steel–concrete composite beams with partial

- interaction: A plastic-hinge approach. *Engineering Structures*, 248, art.number:113256. Available at: <https://doi.org/10.1016/j.engstruct.2021.113256>.
- Lemes, Í.J.M., Silva, A.R.D., Silveira, R.A.M. & Rocha, P.A.S. 2017. Numerical analysis of nonlinear behavior of steel concrete composite structures. *Revista IBRACON de Estruturas e Materiais*, 10(1), pp.53-83. Available at: <https://doi.org/10.1590/S1983-41952017000100004>.
- Lenci, S. & Clementi, F. 2012. Effects of shear stiffness, rotatory and axial inertia, and interface stiffness on free vibrations of a two-layer beam. *Journal of Sound and Vibration*, 331(24), pp.5247-5267. Available at: <https://doi.org/10.1016/j.jsv.2012.07.004>.
- Mechab, I. 2005. *Contribution à l'analyse des plaques stratifiées et sanduricly en utilisant les théories à ordre élevés*. PhD thesis. Oran, Algeria : Université d'Oran1 - Ahmed Ben Bella, Département de Génie Civil [online]. Available at: <https://www.pnst.cerist.dz/detail.php?id=16616> [Accessed: 06 December 2024].
- Mindlin, R.D. 1951. Influence of Rotary Inertia and Shear on Flexural Motions of Isotropic Elastic Plates. *Journal of Applied Mechanics*, 18(1), pp.31-38. Available at: <https://doi.org/10.1115/1.4010217>.
- Nguyen, Q.H. 2009. *Modelling of the nonlinear behaviour of composite beams taking into account time effects*. PhD Thesis. Rennes, France: INSA Institut national des sciences appliquées de Rennes. Available at: <https://doi.org/10.13140/RG.2.1.1706.9923>.
- Oliveira, L.A.M., Borghi, T.M., Rodrigues, Y.O. & El Debs, A.L.H.C. 2021. Assessment of design codes for the in-service behaviour of steel-concrete composite slabs. *Revista IBRACON de Estruturas e Materiais*, 14(5), e14501. Available at: <https://doi.org/10.1590/S1983-41952021000500001>.
- Perkowski, Z. & Czabak, M. 2019. Description of behaviour of timber-concrete composite beams including interlayer slip, uplift, and long-term effects: Formulation of the model and coefficient inverse problem. *Engineering Structures*, 194, pp.230-250. Available at: <https://doi.org/10.1016/j.engstruct.2019.05.058>.
- Reddy, J.N. 1984. A Simple Higher-Order Theory for Laminated Composite Plates. *Journal Applied Mechanics*, 51(4), pp.745-752. Available at: <https://doi.org/10.1115/1.3167719>.
- Reissner, E. 1945. The Effect of Transverse Shear Deformation on the Bending of Elastic Plates. *Journal of Applied Mechanics*, 12(2), pp.A69-A77. Available at: <https://doi.org/10.1115/1.4009435>.
- Santos, H.A.F.A. 2020. Buckling analysis of layered composite beams with interlayer slip: A force based finite element formulation. *Structures*, 25, pp.542-553. Available at: <https://doi.org/10.1016/j.istruc.2020.03.002>.
- Timoshenko, S. & Woinowsky-Krieger, S. 1959. *Theory of Plates and Shells*. McGraw-Hill Book Company. ISBN: 0-07-064779-8.
- Valizadeh, N., Natarajan, S., Gonzalez-Estrada, O.A., Rabczuk, T., Bui, T.Q. & Bordas, S.P.A. 2013. NURBS-based finite element analysis of functionally graded plates: Static bending, vibration, buckling and flutter. *Composite*

*Structures*, 99, pp.309-326. Available at: <https://doi.org/10.1016/j.compstruct.2012.11.008>.

Wang, C.M., Reddy, J.N. & Lee, K. H. 2000. *Shear Deformable Beams and Plates: Relationships with Classical Solutions*. Elsevier Science. Available at: <https://doi.org/10.1016/B978-0-08-043784-2.X5000-X>

Whitney, J.M. 1969. The Effect of Transverse Shear Deformation on the Bending of Laminated Plates. *Journal of Composite Materials*, 3(3), pp.534-547. Available at: <https://doi.org/10.1177/002199836900300316>.

Xu, R. & Wu, Y.-F. 2008. Free vibration and buckling of composite beams with interlayer slip by two-dimensional theory. *Journal of Sound and Vibration*, 313(3-5), pp.875-890. Available at: <https://doi.org/10.1016/j.jsv.2007.12.029>.

Yoo, S.-W., Choi, Y.-C., Choi, J.-H. & Choo, J.F. 2021. Nonlinear flexural analysis of composite beam with Inverted-T steel girder and UHPC slab considering partial interaction. *Journal of Building Engineering*, 34, art.number:101887. Available at: <https://doi.org/10.1016/j.jobe.2020.101887>.

Estudio estático y dinámico de vigas compuestas con un nuevo campo deslizando interlaminar utilizando diferentes teorías de vigas

**Rachida Mohamed Krachai<sup>ab</sup>, Noureddine Elmeiche<sup>a</sup>, autor de correspondencia, Ismail Mechab<sup>c</sup>, Fabrice Bernard<sup>d</sup>, Hichem Abbad<sup>a</sup>**

<sup>a</sup> Universidad Djilali Liabes, Facultad de Tecnología,  
Departamento de Ingeniería Civil y Obras Públicas,  
Laboratorio de Ingeniería Civil y Ambiental (LGCE),  
Sidi Bel-Abbes, República Argelina Democrática y Popular

<sup>b</sup> Universidad Mustapha Stambouli, Facultad de Ciencia y Tecnología,  
Departamento de Ingeniería Civil,  
Mascara, República Argelina Democrática y Popular

<sup>c</sup> Universidad Djilali Liabes, Facultad de Tecnología,  
Departamento de Ingeniería Mecánica,  
Laboratorio de Mecánica y Física de Materiales (LMFM),  
Sidi Bel-Abbes, República Argelina Democrática y Popular

<sup>d</sup> Universidad de Rennes, INSA Rennes,  
Laboratorio de Ingeniería Civil y Mecánica (LGCGM),  
Rennes, República Francesa

CAMPO: ingeniería civil

TIPO DE ARTÍCULO: artículo científico original

#### Resumen:

**Introducción/objetivo:** El presente trabajo tiene como objetivo realizar una investigación estática y dinámica de vigas compuestas por dos elementos conectados entre sí, con una interacción parcial entre las capas de la viga, teniendo en cuenta el efecto de deslizamiento interlaminar.

**Métodos:** En este estudio se ha introducido un nuevo campo de deslizamiento interlaminar que tiene en cuenta, para cada capa, el

*desplazamiento axial, la rotación debida a la flexión y el corte transversal de alto orden con una nueva función de forma de alabeo. Las ecuaciones de equilibrio se resolvieron analíticamente basándose en el principio de Hamilton. Además, la resolución numérica de estas ecuaciones se basó en el principio de minimizar todas las energías utilizando el método de Ritz, teniendo en cuenta diferentes teorías de vigas. Posteriormente se llevó a cabo un estudio comparativo para calcular las frecuencias de vibración naturales de dos vigas compuestas de acero y madera.*

*Resultados: Se encontró que los resultados obtenidos para las diez frecuencias de vibración naturales concuerdan perfectamente con los reportados en trabajos previos encontrados en la bibliografía.*

*Conclusión: Además, se realizó un estudio detallado, dependiendo de los parámetros geométricos y materiales, para los dos materiales mixtos, es decir, hormigón-madera y acero-hormigón, con dos campos de deslizamiento interlaminares, concretamente el campo de deslizamiento clásico basado en la teoría de la viga de Timoshenko y un nuevo campo de deslizamiento interlaminar que se basa en la teoría de orden superior. Además, se estudió la flexión en el caso estático para examinar el efecto de la fuerza cortante interlaminar en vigas cortas y largas.*

*Palabras claves: estudio estático y dinámico, vigas compuestas, interacción parcial, nuevo campo de deslizamiento interlaminar, cortante transversal de alto orden, nueva función de forma de alabeo, método de Ritz.*

Статическое и динамическое исследование композитных балок с новым полем межслойного скольжения с использованием различных теорий изгиба балок

Рашида Мохаммед Крачай<sup>аb</sup>, Нуреддин Эль Михельс<sup>а</sup>, **корреспондент**, Исмаил Мечаб<sup>в</sup>, Фабрис Бернар<sup>г</sup>, Хишам Аббас<sup>а</sup>

<sup>а</sup> Университет Джиллали Лиабес - Сиди-Бель-Аббес, технологический факультет, Департамент гражданского строительства и общественных работ, Лаборатория гражданского строительства и охраны окружающей среды (ЛГСОО), г. Сиди-Бель-Аббес, Алжирская Народная Демократическая Республика

<sup>б</sup> Университет Туши Мустафы Стамбули, факультет науки и технологий, г. Маскара, Алжирская Народная Демократическая Республика

<sup>в</sup> Университет Джиллали Лиабес - Сиди-Бель-Аббес, технологический факультет, кафедра гражданского строительства, Лаборатория механики и физики материалов (МФМ), г. Сиди-Бель-Аббес, Алжирская Народная Демократическая Республика

<sup>г</sup> Реннский университет, INSA Rennes, лаборатория гражданского строительства и машиностроения (LGCGM), г. Ренн, Французская Республика

РУБРИКА ГРНТИ: 67.11.00 Строительные конструкции  
ВИД СТАТЬИ: оригинальная научная статья

**Резюме:**

**Введение/цель:** Целью настоящей статьи является проведение статического и динамического исследования композитных балок, состоящих из двух соединенных элементов с частичным взаимодействием между слоями балки и с учетом эффекта межслойного скольжения.

**Методы:** В данном исследовании было введено новое поле межслойного скольжения, которое учитывает осевое смещение по каждому слою, поворот изгиба и поперечный сдвиг высшего порядка с новой функцией формы изгиба. Уравнения равновесия были решены аналитически, основываясь на принцип Гамильтона. Помимо того, численное решение этих уравнений было основано на принципе минимизации всех энергий с использованием метода Рунца с учетом различных теорий пучков. Затем проведен сравнительный анализ с целью расчета собственных частот колебаний двух композитных балок, изготовленных из стали и дерева.

**Результаты:** Было обнаружено, что результаты, полученные по десяти собственным частотам колебаний, полностью согласуются с результатами, представленными в ранее опубликованных работах.

**Вывод:** Далее было проведено детальное исследование зависимости от геометрических параметров и параметров материалов двух композитных материалов, то есть бетона, дерева и сталебетона с двумя межслойными полями скольжения, а именно, классическим полем скольжения, основанным на теории балок Тимошенко, и новым межслойным полем скольжения, основанным на теории высшего порядка. Помимо того, изгиб был изучен в статическом режиме с целью изучения влияния межслойной силы сдвига на короткие и длинные балки.

**Ключевые слова:** статические и динамические исследования, композитные балки, частичное взаимодействие, новое поле межслойного скольжения, поперечный сдвиг высокого порядка, новая функция формы изгиба, метод Рунца.

Статичко и динамичко проучавање спрегнутих носача са новим интерламинарним смичућим полем коришћењем различитих теорија носача

Рашида Мухамед Крачаи<sup>аб</sup>, Нуредин Елмиш<sup>а</sup>, аутор за преписку,  
Исмаил Метаб<sup>в</sup>, Фабрис Бернар<sup>г</sup>, Етшам Абад<sup>а</sup>

<sup>a</sup> Универзитет „Билали Лиабес“, Технолошки факултет,  
Департман за грађевинарство и јавне радове,  
Лабораторија за грађевинско и еколошко инжењерство (LGCE),  
Сиди Бел Абес, Народна Демократска Република Алжир

<sup>b</sup> Универзитет „Мустафа Стамболи“,  
Факултет науке и технологије, Одсек за грађевинарство,  
Маскара, Народна Демократска Република Алжир

<sup>b</sup> Универзитет „Билали Лиабес“, Технолошки факултет,  
Департман за машинство,  
Лабораторија за механику и физику материјала (LMPM),  
Сиди Бел Абес, Народна Демократска Република Алжир

<sup>г</sup> Универзитет у Рену, ИНСА Рен,  
Лабораторија за грађевинарство и машинство (LGCGM),  
Рен, Француска Република

ОБЛАСТ: грађевинарство

КАТЕГОРИЈА (ТИП) ЧЛАНКА: оригинални научни рад

**Сажетак:**

*Увод/циљ:* У овом раду су статички и динамички проучавани спрегнути носачи састављени од два спојена дела са парцијалном интеракцијом између слојева носача, при чему је узет у обзир ефекат интерламинарног смицања.

*Методе:* Уводи се ново интерламинарно поље смицања које за сваки слој узима у обзир аксијални померај, ротацију услед савијања и попречно смицање високог реда са новом функцијом облика савијања. Једначине равнотеже су решене аналитички на основу Хамилтоновог принципа. При томе је нумеричко решавање ових једначина било засновано на принципу минимизирања свих енергија коришћењем Рицовог метода и различитих теорија носећих греда. Затим је урађена компаративна студија ради израчунавања фреквенција природних вибрација два спрегнута носача од челика и дрвета.

*Резултати:* Утврђено је да су резултати добијени за десет фреквенција природних вибрација у савршеном складу са онима из претходно објављених радова.

*Закључак:* Урађена је детаљна студија на основу параметара геометрије и материјала за два композита (бетон-дрво и челик-бетон) са два интерламинарна поља смицања, односно са класичним пољем смицања на основу теорије греде Тимошенка и са новим интерламинарним пољем смицања на основу теорије високог реда. Савијање је анализирано и статички ради испитивања утицаја интерламинарне силе смицања на кратке као и на дугачке греде.



*Кључне речи: статичко и динамичко испитивање, спрегнути носачи, парцијална интеракција, ново поље интерламинарног смицања, попречно смицање високог реда, нова функција облика савијања, Рицов метод.*

Paper received on: 14.08.2024.

Manuscript corrections submitted on: 30.01.2025.

Paper accepted for publishing on: 31.01.2025.

© 2025 The Authors. Published by Vojnotehnički glasnik / Military Technical Courier (www.vtg.mod.gov.rs, втг.мо.унр.срб). This article is an open access article distributed under the terms and conditions of the Creative Commons Attribution license (<http://creativecommons.org/licenses/by/3.0/rs/>).

